*J. exp. Biol.* **123**, 71–92 (1986)
*Printed in Great Britain* © *The Company of Biologists Limited 1986*



# TRANSCELLULAR AND PARACELLULAR FLOW OF WATER DURING SECRETION IN THE UPPER SEGMENT OF THE MALPIGHIAN TUBULE OF *RHODNIUS PROLIXUS*: SOLVENT DRAG OF MOLECULES OF GRADED SIZE

BY GUILLERMO WHITTEMBURY, ANGELA C. BIONDI*, AZAEL PAZ-ALIAGA†, HENRY LINARES, VALENTÍN PARTHE AND NANCY LINARES

*Centro de Biofísica y Bioquímica, Instituto Venezolano de Investigaciones Científicas, IVIC, Caracas, Venezuela*

*Accepted 3 January 1986*

SUMMARY

The following molecules graded in size were added to the fluid bathing the blind end of the upper segment of the Malpighian tubules of *Rhodnius*: urea (U), erythritol (E), mannitol (M), L-glucose (G), sucrose (S), polyethyleneglycol 800 (PEG), raffinose (R), inulin (I) and dextran 15 000–18 000 (D). U, E, M and G distribute themselves within the cell and the extracellular space, while S, PEG, R, I and D are exclusively extracellular. In addition, the net secretory flow ($J^s_n$) of these probes was studied as a function of the net secretory volume flow ($J_v$). $J^s_n$ is made up of a diffusive component ($J^s_d$), mainly due to unstirred layer effects, and of a convective component ($J^s_c$), due to the drag (entrainment) of the probes by the water flow. The relative contribution of $J^s_d$ and of $J^s_c$ for each probe was studied as a function of $J_v$. It was found that $J^s_c \gg J^s_d$ for U, E, M, G, S and PEG. Therefore these probes are dragged by water. On the other hand $J^s_d = J^s_n$ for R, I and D, which are not entrained. It is concluded that water flows *via* extracellular pathways since S and PEG, which are true extracellular probes, are entrained by solvent. In addition to extracellular pathways, it is suggested that the transcellular structures described by Wessing (1965) and Bergeron *et al.* (1985) could also be the sites of solute–solvent coupling.

## INTRODUCTION

The upper (blind or distal) segment of the Malpighian tubule of *Rhodnius* is known to secrete a fluid isosmotic to that surrounding it, at rates which may

* Present address: Instituto de Química-Física, Facultad de Bioquímica, Química y Farmacia, Universidad Tucumán, San Miguel de Tucumán, Argentina.

† Present address: Departamento de Fisiología, Universidad de San Agustín de Arequipa, Arequipa, Perú.

Key words: paracellular flow, Malpighian tubules, secretion, epithelia.

reach $50\,nl\,cm^{-2}s^{-1}$, in response to stimulation by varying concentrations of diuretic hormone. The action of the latter can be mimicked by 5-hydroxytryptamine (5-HT) (Maddrell, 1969, 1980*a,b*). This secretion is currently thought to be transcellular rather than paracellular (O'Donnell, Aldis & Maddrell, 1982; O'Donnell & Maddrell, 1983; O'Donnell, Maddrell & Gardiner, 1984). Transepithelial water osmotic permeability is of the order of $58\times10^{-4}\,cm^3\,cm^{-2}\,s^{-1}\,osmol^{-1}$, which it is thought can be explained by transcellular flow, without the need to invoke paracellular routes. In addition, the small relative frontal area of the intercellular spaces, i.e. the area facing the apical epithelial surface, as compared to the whole cell area, is also used as an argument against the possibility of paracellular water flow (O'Donnell *et al.* 1982). Similar arguments have been used to dismiss the possibility of paracellular water flow in other isosmotic transporting epithelia (which essentially absorb fluid) (Diamond, 1979; Berry, 1983). However, independent experimental evidence indicates that not only the transcellular, but also the paracellular, routes may be used for water flow during the normal function of these epithelia. Thus, in the proximal renal tubule, the transcellular water osmotic permeability is lower than the transepithelial one, suggesting that there is a significant paracellular water osmotic permeability (Whittembury, 1967; Carpi-Medina, Lindemann, González & Whittembury, 1984; González, Carpi-Medina, Linares & Whittembury, 1984; Whittembury *et al.* 1985). In addition, evidence for the existence of paracellular water flow stems from the observation that water drags some non-electrolytes that are known to be extracellular during absorption in *Necturus* gall bladder (Hill & Hill, 1978), *Necturus* proximal tubule (Berry & Boulpaep, 1964), mammalian gall bladder, *Necturus* and rat proximal tubule (Whittembury, Verde-Martínez, Linares & Paz-Aliaga, 1980; Whittembury *et al.* 1985), rabbit gall bladder (Steward, 1982*a,b*) and mammalian salivary glands (Hunter, Case, Steward & Young, 1982). The existence of solvent drag is deduced in these studies from the observation that the passage of extracellular non-electrolytes is accelerated by the absorptive flow to an extent which unstirred layer effects cannot explain. Pathways for water flow bear on the mechanisms of solute–solvent coupling (Hill, 1975; Hill & Hill, 1978; Diamond, 1979; Berry, 1983; Schafer, 1984).

We decided to explore the possibility that truly extracellular molecules may be dragged by solvent in the Malpighian tubules of *Rhodnius*, which secrete rather than absorb fluid isosmotically. Although it has been dismissed as a possibility (O'Donnell & Maddrell, 1983), the presence of solvent drag of extracellular molecules in this structure would indicate that water could move through the extracellular spaces not only in absorptive epithelia but also in this isosmotically secreting one. In the Malpighian tubules, the permeability of several molecules of graded size has been closely scrutinized (Ramsay, 1958; Maddrell & Gardiner, 1974; O'Donnell *et al.* 1984). It has been clearly established that mannitol (an extracellular marker in other tissues) enters the Malpighian tubule cells, while sucrose and inulin remain extracellular. However, the relationship between transepithelial flow of these molecules and secretory volume flow has not been systematically studied in this preparation, as it has in vertebrate isosmotic transporting epithelia (see above). An additional feature

of the Malpighian tubule is of particular interest for the study of extracellular solvent drag. The morphology of the paracellular route in the Malpighian tubule differs from that of vertebrate epithelia (Lane & Skaer, 1980). In the latter, it is formed by short junctions (<1 $\mu$m in depth) which show *zonulae occludentes, zonulae adhaerentes* and desmosomes (Farquhar & Palade, 1963; Martínez-Palomo & Erlij, 1975), while in the former it is made up of long, smooth septate junctions (Noirot-Timothee, Smith, Cayer & Noirot, 1978; Skaer, Harrison & Lee, 1979). The cells of the Malpighian tubule are about 100 $\mu$m in diameter. In consequence, the total frontal length of junctions per $cm^2$ of epithelium is far smaller than that in mammalian preparations (with cells 10 $\mu$m in diameter). Thus in the *Rhodnius* Malpighian tubule the total length of junctions is 230 cm $cm^{-2}$ of tubular surface, as compared with 2300 cm $cm^{-2}$ in the rabbit proximal tubule (Whittembury, 1967). Finally, the Malpighian tubules can be dissected practically free of connective tissue. Therefore, the evaluation of the space of distribution of the substances used in the solvent drag experiments is free of some problems involved in the estimation of the space of distribution of, for example, the gall bladder, where the connective tissue occupies a space larger than that of the epithelium.

A series of molecules of increasing molecular weights and different shapes was chosen, namely urea, erythritol, mannitol, L-glucose, sucrose, polyethyleneglycol (PEG) $M_r$ 800, raffinose, inulin and dextran $M_r$ 15 000–18 000 to try to explore the geometry of the pathways they would use to permeate the epithelium. The first four molecules penetrate the cells, while the last five are true extracellular markers. The passage of the first six molecules across the epithelium was accelerated by the rate of fluid secretion much more than expected as a result of unstirred layer effects. Therefore, it may be concluded that these molecules are dragged by water. The passage of the last three was accelerated by the secretory flow in a manner that can be entirely explained by unstirred layer effects and not by solvent drag. Since sucrose and PEG are true extracellular probes, the solvent drag of these molecules must be extracellular. Therefore, water must flow through extracellular pathways in addition to the transcellular routes. Part of this work has been published in a preliminary form (Biondi, Linares, Linares & Whittembury, 1982; Paz-Aliaga, Linares & Whittembury, 1983).

## MATERIALS AND METHODS

Fifth instar *Rhodnius prolixus* were used, 1–4 weeks after moulting, from a laboratory culture maintained at 28°C at a humidity of 95%. Upper Malpighian tubules were isolated into drops of insect Ringer solution (see below) under oxygenated, water-saturated liquid paraffin as described by Ramsay (1958) and Maddrell (1969, 1980*a*,*b*). For this purpose, an appropriate chamber was thermostatted at 30°C, the blind end of the tubule was kept immersed near one glass rod, to which an oxygenated Ringer drop with a volume of 0·1–0·5 $\mu$l had been attached under paraffin oil, while the cut end was tied up around another glass rod. These small-sized drops were renewed every 2–5 min. They were chosen in order to achieve

appropriate molecular self-stirring of the bathing solution. A sphere of 0·1–0·5 $\mu$l has a radius (300–500 $\mu$m) critical for self-stirring. The time delay for 90 % equilibration by diffusion can be calculated [using equation 143 (Jacobs, 1935) or equation 6.20 (Crank, 1956)] to be 8 s and 22 s for the 300- and 500-$\mu$m-radius drops, respectively. Since our collections were usually performed at intervals of at least 5 min there should have been ample time for mixing. The Ringer solution contained 1 mmol $l^{-1}$ of the probing molecule. At time $t = 0$, secretion was started by addition to the Ringer solution of 5-HT to a concentration which varied from $10^{-5}$ to $10^{-7}$ mol $l^{-1}$. Periodic collection of the secretion was performed with techniques for handling small volumes (Shipp *et al.* 1958). Collections lasted for about 2 h. Samples were used once the secretory rate stabilized.

The rate of secretion, $J_v$, was calculated from the volume and duration of collection and the area of tubular surface exposed to the Ringer solution. The area was obtained from *camera lucida* tracings to measure tubular length. It was assumed that the tubules were well represented by a cylinder. An image splitter was used to evaluate tubule diameters (Carpi-Medina *et al.* 1984). $J_v$ was expressed in nl $cm^{-2}$ $s^{-1}$. The volume of each collection was directly pipetted into 1 ml of distilled water and counted with 3 ml of counting solution in a Packard 3000 liquid scintillation counter. Known volumes of Ringer were similarly counted.

$J_n^s$, the rate of secretion per unit bath concentration ($C_1$), was calculated as $J_v \times C_2/C_1$, where $C_2$ is the concentration of the radioactive substance in the secreted fluid. $J_n^s/C_1$ has units of nl $cm^2$ $s^{-1}$.

The Ringer solution has the following composition (Maddrell, 1969, 1980*a*,*b*) in mmol $l^{-1}$: NaCl, 129; KCl, 8·6; $NaH_2PO_4$, 4·3; $NaHCO_3$, 10·2; $CaCl_2$, 2·0; glucose, 34; alanine, 3. The pH was 7·35–7·45 and the osmolality 340 mosmol $kg^{-1}$, as measured by the freezing point method. The chemicals were from E. Merck, Darmstadt, except dextran (Sigma Chemical Co.). The following radioactive substances (New England Nuclear Corp.) were used: [$^{14}$C]urea, [$^{14}$C]mannitol, [$^{3}$H]L-glucose, [$^{14}$C]sucrose, [$^{3}$H]raffinose, [$^{3}$H]polyethyleneglycol 800, [$^{14}$C]-inulin, [$^{14}$C]dextran. Enough counts of these substances in 1 mmol $l^{-1}$ carrier were added to the Ringer solution drop that bathed the tubule. Chromatographic runs indicated that these substances had not hydrolysed.

*Distribution of molecules in tissue spaces*

The tubules were treated as described above. Samples were obtained to measure the secretion concentration ($C_2$) and the bath concentration ($C_1$) of the probing molecules. The tubules were then taken out of the bath with a glass hook. They were then quickly immersed for 1 s in each of three Ringer baths (10 $\mu$l each). This removed at least 95 % of the radioactive counts outside the tubule. The tubules were then dipped in 1 ml of water in a counting vial. Aliquots of the secreted and bathing solutions were also counted. From the lumen volume ($V^L$) and concentration of the probing molecule ($C_2$), the probing molecule tubular lumen content ($C^L$) was calculated. The tissue content ($C^T$) (as determined from the radioactive counts in the tissue) minus the lumen content gave the cell content $C^c$ which, divided by the cell

Table 1. *Space of distribution of the probing molecules (S) during secretion*

| Probing molecule | $M_r$ | $r_m$ (nm) | $S$ |
|---|---|---|---|
| Urea | 60 | 0·23 | 94 ± 8 |
| Erythritol | 122 | 0·32 | 68 ± 7 |
| L-Glucose | 180 | 0·4 | 58 ± 9 |
| Mannitol | 182 | 0·4 | 62 ± 6 |
| Sucrose | 342 | 0·45×0·48 | 4·6 ± 0·2 |
| Raffinose | 594 | 0·57×0·6 | 4·0 ± 0·9 |
| Polyethylene glycol (PEG) | 800 | 0·34×1·85 | 5·0 ± 0·2 |
| Inulin | 5000 | 0·6×(9–12) | 5·2 ± 1·0 |
| Dextran | 15 000–18 000 | 1·4×30 | 6·9 ± 0·2 |

$S$ is expressed as percentage of the Malpighian tubule cell volume: mean ± S.E.M., $N = 6$.

The tubules have a 0·5 μm thick extracellular basal material (Figs 6, 7) which makes up 6 % of the cell volume, $V^c$. The average $V^c = 14\,nl\,cm^{-1}$ (tubular external diameter = 55 μm; lumen diameter = 35 μm).

Relative molecular mass, ($M_r$). Molecular radii ($r_m$) in nm were measured in molecular models except for inulin (Phelps, 1965) and dextran (Renkin, 1970).

volume, $V^c$, gave the concentration, $C_3$. The space of distribution $S = C_3/C_1$. $S$ is the fraction of $V^c$ occupied by the probe under the assumption that the latter is not concentrated by some subcellular fraction. The probe distributes in the whole tubular cell structure if $S = 1·00$ and it does not enter the cell interior if $S = 0·00$. $V^L$ was calculated from the average lumen diameter (35 μm) and $V^c$ from the average external tubule diameter (55 μm), assuming that the tubules are well represented as cylinders. Thus $V^L = 9·6$ and $V^c = 14·1\,nl\,cm^{-1}$ tubule length (Table 1).

### *Electron microscopy*

After dissection, the upper tubules were used immediately. They were stimulated to secrete with 5-HT as indicated above. After 30 min, the bathing fluid was changed to a glutaraldehyde fixative (100 ml of the basic fixative contained 1 g of glutaraldehyde plus 10 ml of insect Ringer buffered with phosphate buffer to pH 7·3–7·4). The osmolality of the fixative was adjusted to 340 mosmol $kg^{-1}$. After 15–20 min, 1-mm long pieces of tubule were immersed in the same fixative and left overnight at 4°C. After being washed in buffer they were post-fixed in Na-cacodylate-buffered 2 % $OsO_4$ solution (10 mg $ml^{-1}$), dehydrated in acetone, washed in propylene oxide and embedded in Epon 812 (Whittembury & Rawlins, 1971; Whittembury & Hill, 1982). Pale gold to silver sections were stained with uranyl acetate and lead citrate, and examined in a Siemens Elmiskop 1A electron microscope.

## RESULTS

Urea, erythritol, mannitol and L-glucose distribute themselves in most of the intracellular space, while sucrose, raffinose, PEG, inulin and dextran occupy about 5 % of the tissue space. The peritubular extracellular matrix is 0·5 μm thick (Figs 6, 7), which is about 6 % of the cell space, which is 14 nl $cm^{-1}$ length (lumen excluded,

see footnote to Table 1). Assuming that the intercellular spaces are 0·1 μm wide, it can be calculated that the tissue intercellular space would be 0·23 % of the tissue volume. These observations warrant the use of sucrose, raffinose, PEG, inulin and dextran as extracellular substances in the Malpighian tubule upper segment. Urea, erythritol, L-glucose and mannitol must certainly cross the cell in addition to distributing themselves in the extracellular space.

Figs 1–4 and Table 2 summarize the relationship between the net secretory flux of the probing molecules (per unit bath concentration), $J_n^s/C_1$, and $J_v$, the secretory flow rate. Although more complex functions may also fit the data, the straight line is the simplest fit, with a very high correlation coefficient for urea, erythritol, mannitol, L-glucose, sucrose and PEG. Fig. 5 gives the ratio $C_2/C_1$ as a function of the relative molecular mass of the probing molecules for three rates of $J_v$.

For urea, erythritol, L-glucose, mannitol, sucrose and PEG, the dashed (diffusion) line is statistically different from the line representing the experimental values (Figs 1–3; Table 2).

Since the relationship between $J_n^s/C_1$ and $J_v$ for raffinose and dextran is not statistically significant, no regression line has been drawn (Fig. 4). Inulin shows a regression line with a slope significantly different from zero (Fig. 4). However, the distribution of none of these three substances is different from the distribution expected from diffusion due to unstirred layer effects because the dashed line and the experimental values coincide (Table 2). Fig. 5 shows the relationship between

Table 2. *Regression parameters of net solute (secretory) flux per unit bath concentration ($J_n^s/C_1$) studied as a function of net (secretory) volume flow ($J_v$) in the Malpighian tubule distal segment*

| Probing molecule | $r$ | b | m | $P$ | $N$ | $P_0^s$ | $\sigma$ | $P^*$ |
|---|---|---|---|---|---|---|---|---|
| Urea | 0·99 ± 0·03 | 2·04 ± 0·53 | 0·81 ± 0·03 | <0·001 | 22 | 2·9 | 0·10 | 0·001 |
| Erythritol | 0·98 ± 0·04 | 0·41 ± 0·32 | 0·82 ± 0·04 | <0·001 | 20 | 2·8 | 0·15 | 0·001 |
| L-Glucose | 0·87 ± 0·08 | 0·32 ± 0·18 | 0·21 ± 0·02 | <0·001 | 44 | 2·3 | 0·68 | 0·005 |
| Mannitol | 0·71 ± 0·12 | 1·58 ± 0·057 | 0·19 ± 0·04 | <0·001 | 27 | 2·6 | 0·70 | 0·01 |
| Sucrose | 0·89 ± 0·09 | 0·20 ± 0·06 | 0·04 ± 0·004 | <0·001 | 31 | 0·17 | 0·90 | 0·001 |
| Raffinose | 0·11 ± 0·16 | 0·27 ± 0·06 | 0·003 ± 0·004 | NS | 42 | 0·15 | 1·00 | NS |
| Polyethylene glycol (PEG 800) | 0·95 ± 0·07 | 0·07 ± 0·04 | 0·05 ± 0·003 | <0·001 | 22 | 0·13 | 0·91 | 0·001 |
| Inulin | 0·28 ± 0·20 | 0·36 ± 0·08 | 0·015 ± 0·011 | NS | 26 | 0·13 | 1·00 | NS |
| Dextran | 0·42 ± 0·18 | 0·19 ± 0·19 | 0·05 ± 0·02 | 0·02 | 27 | 0·10 | 1·00 | NS |

Data displayed in Figs 1–4 were fitted by least squares to an equation of the form $(J_n^s/C_1) = mJ_v + b$, where $m = (1-\sigma)(1+C_2/C_1)/2$ and $b = P_0^s(1-C_2/C_1)$ (see equation 1). b and $P_0^s$ have units of $10^{-6}$ cm s$^{-1}$.

$r$ is the correlation coefficient; $P$ is the probability that the slope is different from 0; $N$ is the number of experiments; $P_0^s$ is the permeability to s when $J_v = 0$; $\sigma$ is the apparent reflection coefficient calculated at high $J_v$ values from m. $P^*$ is the probability that the difference between the slope m and the dashed line of Figs 1–4 (representing the diffusive flow $J_d^s$, equation 2) is significant.

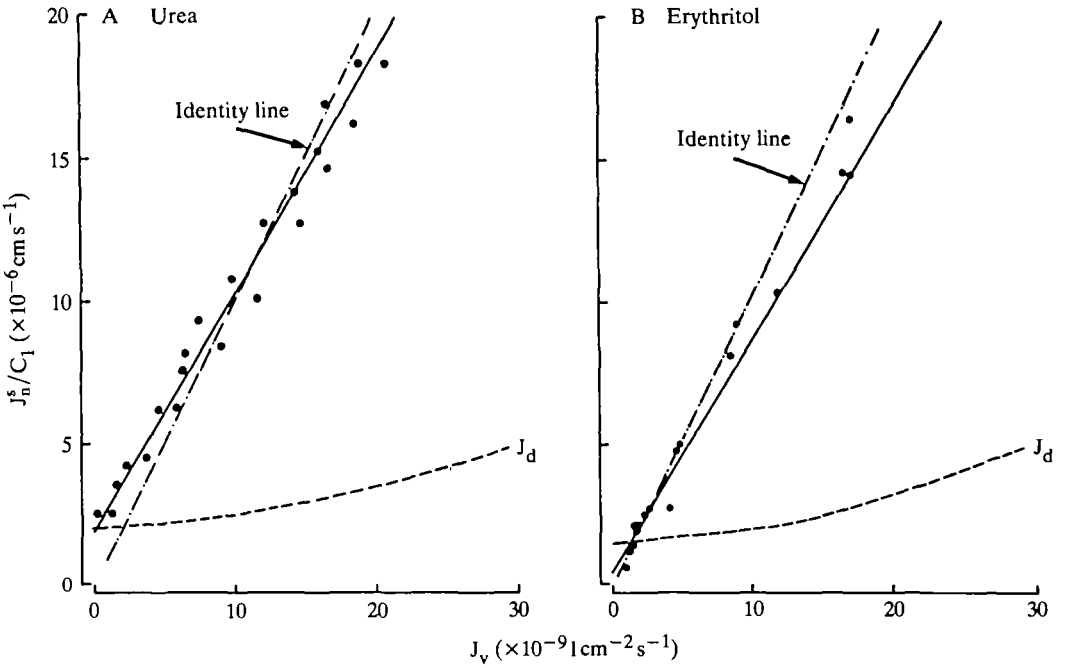


Fig. 1. Net secretory urea (A) and erythritol (B) flux (bath to lumen) per unit bath concentration ($J_n^s/C_1$) as a function of net secretory volume flow ($J_v$) in the Malpighian tubule distal segment. In Figs 1–4, the continuous line represents the regression line, $J_n^s/C_1 = mJ_v + b$, fitted by least squares to the data (Table 2). The dotted-dashed line is the identity line which would obtain if $C_2/C_1 = 1$. The dashed line (denoted $J_d$) represents the diffusive component of $J_n^s/C_1$, calculated using equation 2, as explained in the text. In a given tubule, $J_v$ varied spontaneously after 5-hydroxytryptamine (5-HT) addition. In addition, $J_v$ was varied by using 5-HT concentrations ranging from $10^{-5}$–$10^{-7}$ mol l$^{-1}$ in different tubules.

$C_2/C_1$ and $M_r$ of the probing molecules. $C_2/C_1$ decreases progressively as $M_r$ increases, as Ramsay (1958) and Maddrell & Gardiner (1974) observed. Fig. 5 also illustrates that $C_2/C_1$ ratios decrease as $J_v$ increases.

Thin section electron micrographs (Figs 6, 7) show normal tubular appearance (Wigglesworth & Salpeter, 1962). In addition, structures may be observed that extend from basolateral infoldings to the apex of the cell in the form of parallel lines. These structures, previously described by Wessing (1965), seem to be open at both cell ends. These observations agree with recent observations using thick sections and high voltage electron microscopy (Bergeron *et al.* 1985).

## DISCUSSION

The first task of the present work was to study the space of distribution of probing molecules of increasing molecular weight to differentiate truly extracellular probes from those that penetrate the cell membrane. The Malpighian tubule upper segment is particularly suited for this purpose since it is surrounded by only about 6% of extracellular material (Figs 6, 7). Urea, erythritol, mannitol and L-glucose do

penetrate the cell membrane (Table 1) in agreement with observations indicating that methyl glucose, mannitol and erythritol enter the intracellular space (O'Donnell *et al.* 1984). In contrast, sucrose, PEG, raffinose, inulin and dextran occupy only some 5% of the tubular volume (lumen subtracted). Therefore, these substances must be true extracellular markers, in agreement, again, with observations of O'Donnell *et al.* (1984) for inulin and sucrose. The $C_2/C_1$ ratio shows an inverse relationship with the $M_r$ of the probing molecules (Fig. 5), in agreement with observations of Ramsay (1958), Maddrell & Gardiner (1974) and O'Donnell *et al.* (1984). In addition, the ratio $C_2/C_1$ varies inversely with $J_v$, $C_2/C_1$ ratios being higher at low $J_v$ values and lower at high $J_v$ values (Fig. 5).

*Solvent drag, unstirred layer effects and permeability changes*

A second observation of the present work is the relationship between the net secretory flux per unit bath concentration, $J_n^s/C_1$, of several of the probing molecules and $J_v$. Recalculation of the work of Ramsay (1958) on the stick insect and of

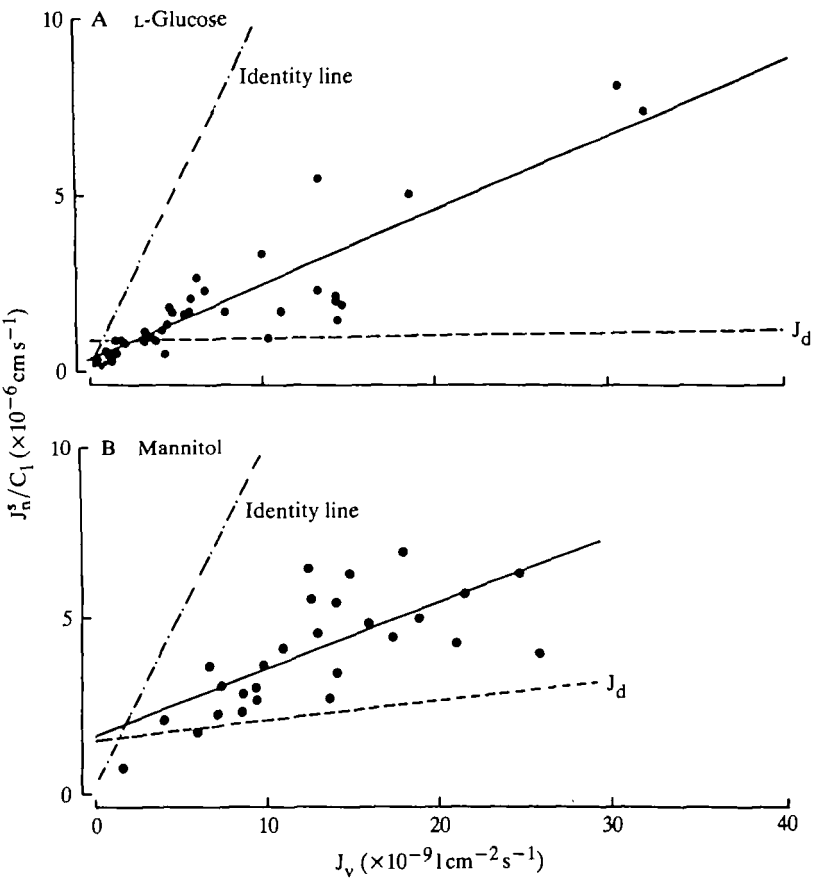


Fig. 2. Net secretory L-glucose (A) and mannitol (B) flux per unit bath concentration, as a function of $J_v$. See Fig. 1 for further details.

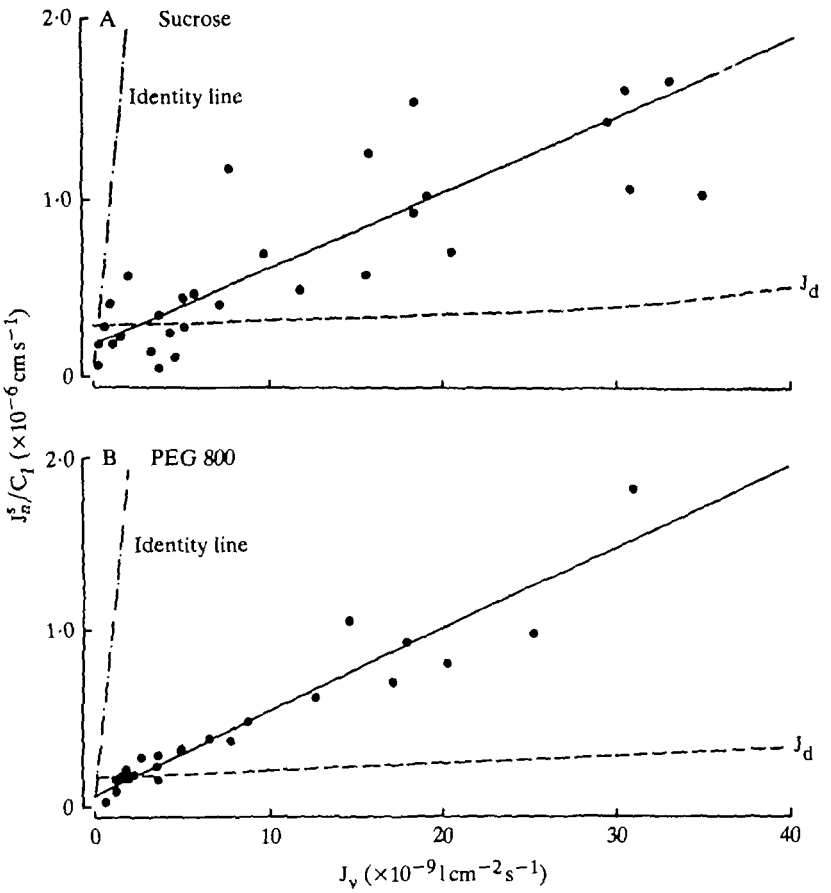


Fig. 3. Net secretory sucrose (A) and polyethylene glycol (PEG 800) (B) flux per unit bath concentration, as a function of $J_v$. The scale of the ordinate is different from that of Figs 1 and 2. See Fig. 1 for further details.

O'Donnell *et al.* (1984) on *Rhodnius* Malpighian tubules shows that this relationship was also present in their experiments. Thus Ramsay studied the excretion of urea and sucrose, among other probes. The rate of urine flow ($R$) (similar to $J_v$) and the probing molecule concentration in the secreted fluid ($C_2$) and in the bathing fluid ($C_1$) may be used to construct a plot of $(C_2 \cdot R/C_1)$ *vs* $R$ which shows a highly significant correlation, with experimental points falling around the identity line for urea, as in Fig. 1 of the present work. A similar plot for sucrose using the data from tables 4, 7 and 8 of Ramsay (1958) also shows a statistically significant positive slope relating $C_2 \cdot R/C_1$ as a function of $R$.

The relationship between $J_n^s/C_1$ and $J_v$ may be analysed with the help of equations 1 (Kedem & Katchalsky, 1958)

$$J_n^s/C_1 = (J_d^s/C_1) + (J_c^s/C_1) \tag{1a}$$

and

$$J_n^s/C_1 = P_0^s \cdot \Delta C^s/C_1 + (1 - \sigma)\, C^{**} J_v/C_1, \tag{1b}$$

where $J_n^s$ is the net flow of solute s (positive in the secretory direction), $P_0^s$ is the permeability to s when $J_v = 0$ ($J_v$ is the net volume flow positive in the secretory direction), $\Delta C^s$ is the transepithelial concentration difference, $\sigma$ is the reflection coefficient of the membrane to s, $C^{*s}$ is the average concentration of s in the membrane and $C_1$ is the concentration of s in the bath.

The first term on the right-hand side of equations 1, $J_d^s/C_1 = P_0^s \cdot \Delta C^s/C_1$, describes the solute flow due entirely to diffusion. The second term, $J_c^s/C_1 = (1-\sigma)C^{*s}J_v/C_1$, indicates the magnitude of the flow of s due to convection, i.e. due to the drag of s by the solvent. Comparison of equation 1b and the regression

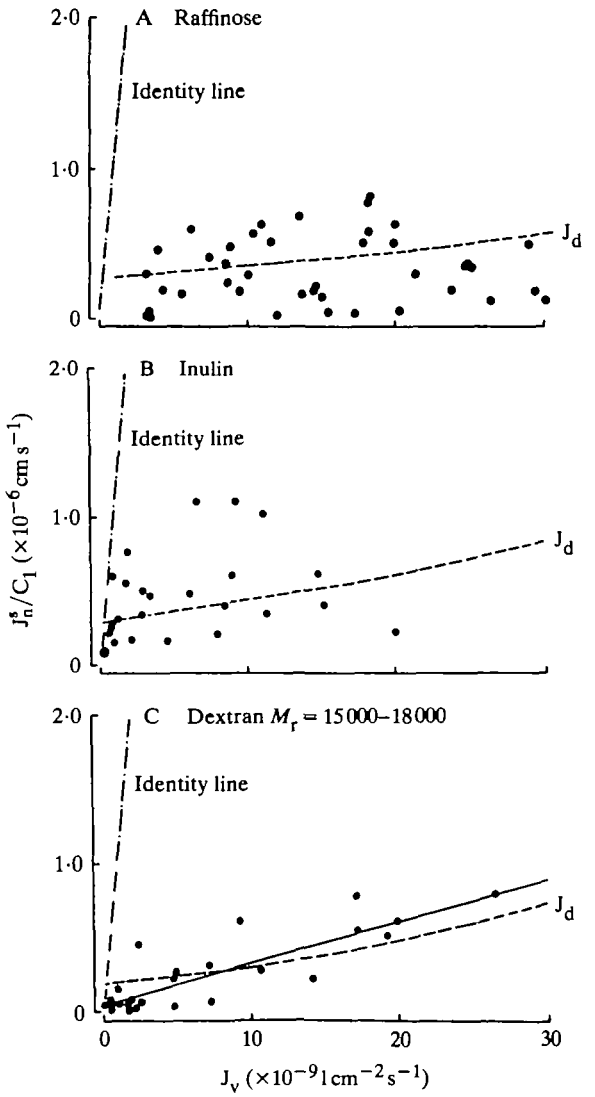


Fig. 4. Net secretory raffinose (A), inulin (B) and dextran (C) fluxes per unit bath concentration as a function of $J_v$. In A and B the correlation between $J_n^s/C_1$ and $J_v$ is not significant and thus no regression line is drawn. See Fig. 1 for further details.

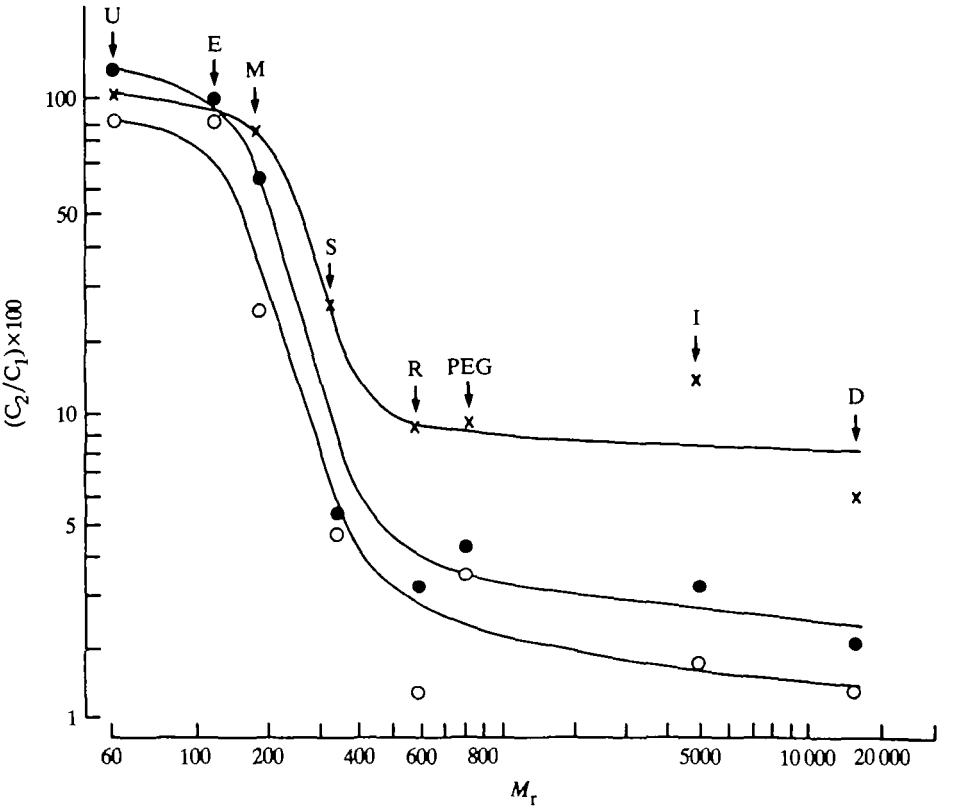


Fig. 5. Ratio of secreted fluid concentration to bath concentration $[(C_2/C_1)\times100]$ plotted as a function of the relative molecular mass ($M_r$) of the probing molecules. $C_2/C_1$ ratios have been averaged at three different $J_v$ values, namely $<5$ nl cm$^{-2}$ s$^{-1}$ (×); from 5 to 15 nl cm$^{-2}$ s$^{-1}$ (●) and $>15$ nl cm$^{-2}$ s$^{-1}$ (○). Lines following the data have been drawn by eye. U, urea; E, erythritol; M, mannitol; S, sucrose; R, raffinose; PEG, polyethylene glycol; I, inulin; D, dextran.

lines for Figs 1–4 (where $J_n^s/C_1 = mJ_v+b$, see legend to Table 2) indicates that $b = P_0^s(C_2-C_1)/C_1$. $P_0^s$ was calculated from the average value for $J_n^s$ at $J_v$ values $<3$ nl cm$^{-2}$ s$^{-1}$ (Figs 1–4) and the actual $C_2/C_1$ ratios, rather than from the intercept b, since no $C_2/C_1$ ratios at $J_v = 0$ can actually be obtained. The slope is given by

$$m = (1-\sigma)C^{**}/C_1 = (1-\sigma)(1+C_2/C_1)/2.$$

It may be seen (Fig. 5) that $C_2/C_1$ ratios vary as a function of $J_v$. Therefore, $\sigma$ would apparently vary as a function of $J_v$. As a matter of fact, useful $\sigma$ values can only be obtained as the highest values of $J_v$ are approached, from $\sigma = 1-2m/(1+C_2/C_1)$. These values are given in Table 2 ($\sigma$ values calculated at low $J_v$ figures can be artefactual; Renkin, 1985).

*Unstirred layer effects*

A relationship between $J_n^s/C_1$ and $J_v$ may be taken to indicate solvent drag but there are circumstances where the above relationship is present due to unstirred layer

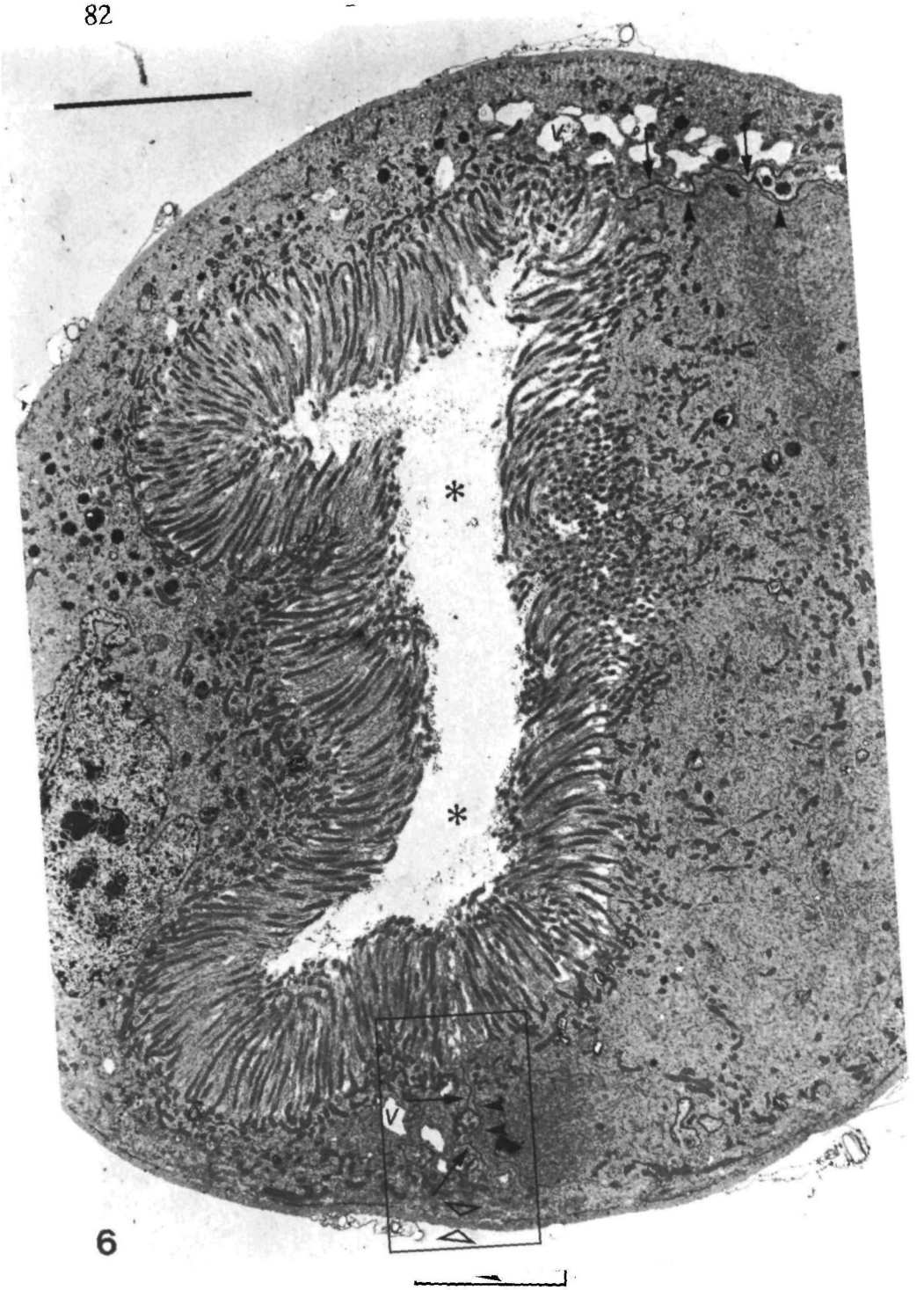


Fig. 6. Cross section of the upper segment of *Rhodnius prolixus* Malpighian tubule. Asterisks denote the tubular lumen; large arrowheads indicate the thickness of the basement membrane, and *v*, vacuoles. Two cells make up one tubular circumference. Microvilli, nuclear material and intracellular organelles show their normal appearance. Despite the small magnification, double-lined structures (small arrowheads) within the cell may be noticed parallel to the intercellular junctions (arrows). These are further illustrated in Fig. 7. Scale bar, 10 $\mu$m.

effects (Andreoli, Schafer & Troutman, 1971; Barry & Diamond, 1984). In the absence of unstirred layers, $\Delta C^s$ equals the secreted fluid ($C_2$) minus bath ($C_1$) concentration difference, $\Delta C^s = C_2 - C_1$. However, with unstirred layers and a significant $J_v$ the movement of water will pile up solute towards side 1 of the membrane (so that the solute concentration at the membrane $C_1' > C_1$) and will wash out solute from side 2 of the membrane (so that the solute concentration at the membrane $C_2' < C_2$). Under these circumstances $\Delta C^s = (C_2' - C_1') > (C_2 - C_1)$. In consequence, not only $J_c^s$ but also $\Delta C^s$ is a function of $J_v$, and therefore $J_d^s/C_1$ is also a function of $J_v$ as expressed by equation 2 (Andreoli *et al.* 1971, equation 12; Barry & Diamond, 1984, equation 83):

$$J_d^s/C_1 = [e^{A'} - (C_2 e^{-A''}/C_1)]/[(1/P_0^s) + (1/J_v)(e^{A'} - e^{-A''})]. \quad (2)$$

The magnitude of $J_d^s$ depends directly on the magnitude of A′ and A″ (since for small x, $e^x = 1+x$) where $A' = J_v d'/D_s$ and $A'' = J_v d''/D_s$. d′ and d″ are the unstirred layer thicknesses at the bath and secretory fluid, respectively (in our case 500 $\mu$m and 17·7 $\mu$m, respectively) taken from the bathing fluid drop radius and the tubular lumen radius, respectively (see Materials and Methods), and $D_s$ is the diffusion coefficient of s. The other terms have already been described.

We have used this equation to calculate $J_d^s$ as a function of $J_v$ for the probes as shown by the dashed lines of Figs 1–4 with (a) values for d′ and d″ of 2×500 $\mu$m and 2×17·5 $\mu$m (i.e. values twice the unstirred layer thicknesses of the bath and secretory side, respectively, to be on the safe side), (b) $P_0^s$ values as given in Table 2, (c) $J_v$ values of 0, 5, 10, 15, 20, 15 and 30 nl cm$^{-2}$ s$^{-1}$ and the corresponding experimental $C_2/C_1$ ratios. The dashed line interpolates the values obtained at 5 nl cm$^{-2}$ s$^{-1}$ intervals of $J_v$.

In Figs 1–4 the solid lines represent the total observed flow, $J_n^s/C_1$ (with slope values shown in Table 2). The differences between the slopes of the solid and the dashed lines give the convective flows ($J_c^s/C_1$). The probability that this difference is statistically significant is shown as $P^*$ in Table 2. If the continuous and the dashed lines are not statistically different, any relationship between $J_n^s/C_1$ and $J_v$ is due to the contribution of $J_d^s$, i.e. to unstirred layer effects. $P^*$ in Table 2 is non-significant for raffinose, inulin and dextran. This indicates that the increase in secretory flow of raffinose, inulin and dextran as a function of $J_v$ can be entirely explained by unstirred layer effects (Fig. 4). Inspection of equations 1 and 2 helps to clarify the relative changes in the weight of $J_d^s$ and $J_c^s$ as a function of $M_r$, the probe relative molecular mass. It is known that the diffusion coefficient, $D_s$, of the probing molecule is inversely related to $M_r$. For example $D_s$ for sucrose, raffinose, PEG, inulin and dextran are, respectively, 6, 4·3, 2·6, 1·8 and 0·9×10$^{-6}$ cm$^2$ s$^{-1}$. In consequence, the unstirred layer effects (which are inversely proportional to $D_s$) and the relative importance of $J_d^s$ will be larger with the larger probes than with the smaller ones, provided $P_0^s > 0$. On the other hand, the weight of $J_c^s$ decreases the larger the probe, because the value of $\sigma$ approaches 1, and $1-\sigma$ approaches 0.

Figs 1–3 show that for urea, erythritol, L-glucose, mannitol, sucrose and PEG the convective component (i.e. $J_n^s/C_1 - J_d^s/C_1$ is highly significant, Table 2).

Obviously, for the molecules entrained by water at $J_v = 0$, $J_d^s \gg J_c^s = 0$. As $J_v$ increases, the convective component becomes progressively more important until at $J_v > 15\,nl\,cm^{-2}s^{-1}$, $J_c^s \gg J_d^s$.

By contrast, it is illustrative to calculate the concentration difference that would be required to explain exclusively by diffusion the net solute flows observed in Figs 1–3 at high $J_v$ values. In the case of urea, erythritol, mannitol, L-glucose, sucrose and PEG, the values for $J_n^s$ at $J_v = 20$–$30\,nl\,cm^{-2}s^{-1}$ are 5–10 times higher than at low $J_v$ values. Therefore, a concentration difference of 5–10 mmol $l^{-1}$ would be required to explain the observed net solute fluxes at high $J_v$ values (instead of the concentration difference of 1 mmol $l^{-1}$, originally set up). These concentration differences cannot be maintained in the small bathing fluid drops used in the present work because self-stirring should counterbalance within a few seconds any tendency to solute accumulation (see Materials and Methods). In other words, 5–10 mm diameter drops would be required to explain by unstirred-layer effects the experimental results shown in Figs 1–3.

*Permeability changes as a function of $J_v$*

Examination of equation 1b indicates that changes in $P_0^s$ as a function of $J_v$ could also result in an increase in $J_n^s$ as a function of $J_v$. It is possible that faster fluid secretion leads to a higher intraluminal hydrostatic pressure which in turn might lead to changes in $P_0^s$. O'Donnell *et al.* (1984) showed that increasing fluid perfusion rates along the lumen of cannulated tubules produced increased rates of sucrose penetration very similar to those produced by similar changes in the rate of fluid secretion across the epithelial wall. Although we do not know the exact explanation for these, we believe that the possibility that $P_0^s$ has increased in our experiments is remote for the following reasons. (1) By definition, $P_0^s = D_s A/A_0 \Delta x$, where $A/A_0$ is the pathway area per $cm^2$ of epithelium, $\Delta x$ is the pathway length and $D_s$ the solute diffusion coefficient. Therefore, an increase in $P_0^s$ is expected if the geometry of the pathways changes. At high $J_v$ values, $J_n^s$ for sucrose is 5–10 times the $J_n^s$ value obtained at low $J_v$ (Fig. 3). To explain that a five- to tenfold increase in $P_0^s$ for sucrose (with a molecular radius of 0·45 nm) is due to geometrical changes, one requires either a five- to tenfold decrease in $\Delta x$ (which is remote) or a five- to tenfold increase in $A/A_0$. The latter would require that the frontal area of the intercellular clefts increases five- to tenfold (either in length or in width). Just a twofold increase in width means a change in width from a slit with a half-width of 0·6 nm (Fig. 8) to one of 1·2 nm. Such a pathway would easily let through raffinose, with a molecular radius of 0·59 nm, which is not the case, since raffinose is retained by the epithelium (Fig. 4). (2) $\sigma$ may be defined as $1-(J_n^s/J_v C^{*s})$; i.e. $\sigma$ is equal to the amount of solute that does not sift through the membrane per unit time divided by the amount arriving at the membrane during that time (Whittembury *et al.* 1980; Renkin, 1985). For sucrose, $\sigma = 0{\cdot}90$ at high $J_v$ values and 0·89 at $J_v = 5\,nl\,cm^{-2}s^{-1}$ and for PEG, $\sigma = 0{\cdot}91$ and 0·89, respectively. If the changes in $J_n^s$ were due to increases in $P_0^s$, and therefore to increases in the pathway area, $\sigma$ should decrease at high $J_v$ values,

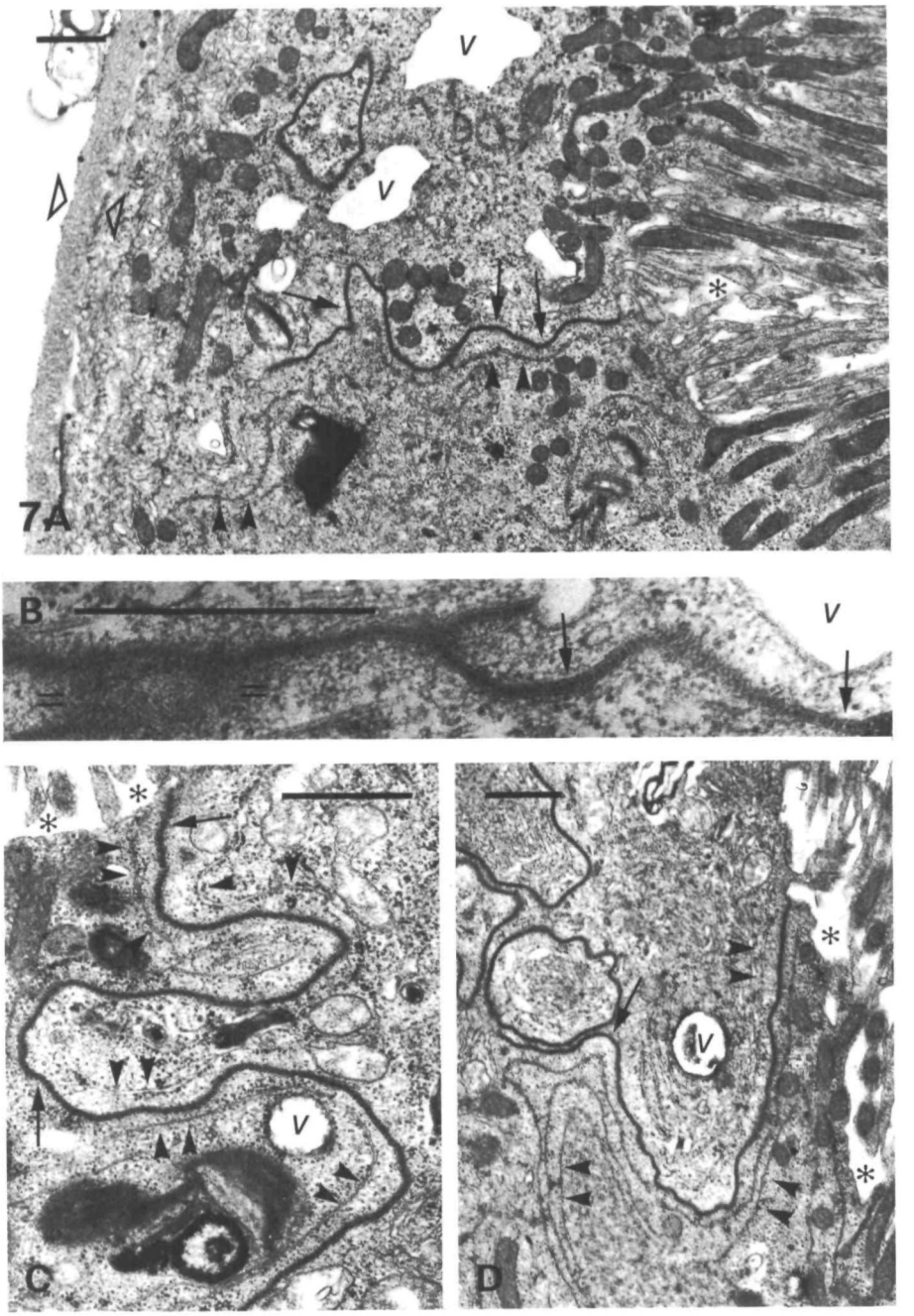


Fig. 7. Upper segment of *Rhodnius prolixus* Malpighian tubules. (A) Higher magnification of the section marked in Fig. 6 (rotated through 90°). (B),(C) and (D) Details of smooth intercellular septate junctions. Notice the fingerprint appearance (= =). Arrowheads in A,C and D show intracellular double-lined structures running from apex to base of the cell. Arrows indicate intercellular junctions. Scale bar, 1 $\mu$m. *v*, vacuoles.

since $\sigma$ also depends on the geometry of the pathways (see 3, below). The observation that $\sigma$ does not significantly change with $J_v$ argues against possible changes in the geometry of the pathways used by the solute to cross the preparation. (3) Alternatively, one can calculate the magnitude of the change in $A/A_0$ of the pathway that would allow solvent drag of raffinose, so that $\sigma$ for raffinose would be 0·90 (instead of the experimental finding of 1·00), i.e. similar to the values observed for sucrose and PEG (which have $\sigma = 0{\cdot}9$). This calculation can be undertaken using the following equation (equations A11a and A15 of Renkin & Curry, 1979) for slits:

$$1 - \sigma = (1 - 1{\cdot}5a^2 + 0{\cdot}5a^3)(1 - 0{\cdot}333a^2),$$

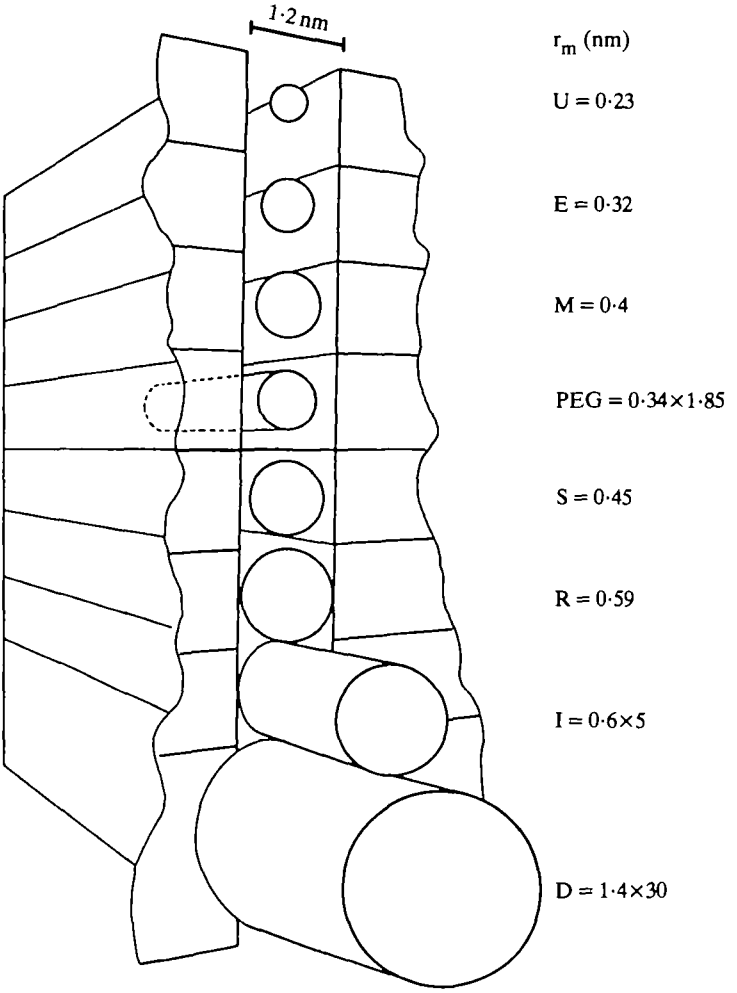


Fig. 8. A 1·2 nm wide slit is compared with the molecular dimensions of the probing molecules. U, E, M, G, PEG, R, I and D stand for urea, erythritol, mannitol, L-glucose, polyethylene glycol $M_r$ 800, sucrose, raffinose, inulin and dextran $M_r$ 15 000–18 000. U, E, M, H, S, R are quasispherical; PEG, I and D are rod-like molecules with major-to-minor axis ratios of about 5, 15–18 and 21, respectively. They are shown with the end of the molecules facing the slit (see text).

where $a = r_m/r_p$, the ratio of the molecular radius, $r_m$, to the radius or half-width of the slit. For $\sigma = 0{\cdot}90$, a turns out to be 0·9 and $r_p = 0{\cdot}65$ nm for a slit (and 0·75 nm for a pore). In other words, just an increase in the slit width to 0·65 nm would let as much raffinose through by convection as the presently calculated slit of 0·5 nm (and a pore of 0·57 nm, see below) lets through sucrose and PEG. Now, since $J_n^s$ for raffinose does not increase markedly with $J_v$, the slit width must have changed to less than 0·65 nm, which – as mentioned in points 1 and 2 – is insufficient to explain the observed increase in $J_n^s$ for sucrose and PEG by diffusion.

One must therefore conclude that urea, erythritol, L-glucose, mannitol, sucrose and PEG are entrained by water. Sucrose and PEG must be dragged by water exclusively, following extracellular pathways, while urea, erythritol, L-glucose and mannitol must be dragged by water following extracellular pathways; they may also be dragged through the cells, although their transcellular movement could mainly be diffusive.

The results shown in Figs 1–4 seem related to the $M_r$ of the probe; raffinose ($M_r$ 594), inulin ($M_r$ 5000) and dextran ($M_r$ 15 000–18 000) are not entrained, whereas the smaller molecules are dragged by water. However, this argument does not apply to PEG ($M_r$ 800), since this is dragged while raffinose, for example, is not. Do steric factors play a role in this discrimination of the epithelium against the probing molecules? Urea, erythritol, mannitol, L-glucose, sucrose and raffinose are quasi-spherical, while PEG, inulin and dextran are long, rod-like molecules with major-to-minor axis ratios of about 5, 15–18 and 21, respectively. Rod-like solute particles in solution flow are oriented by the hydrodynamic forces such that their major axis will tend to be parallel to the direction of the stream lines, due to the fact that the velocity of the solvent in relation to the particle surface is higher at the middle of the molecule than at its ends and is exerted in a direction parallel to the molecule long axis (Schlichting, 1979). When entering a pore-like structure, they will be inserted end-on into it (Cerf & Scheraga, 1942; Nozaki, Schechter, Reynolds & Tanford, 1976). If this criterion is applied, the discrepancy between the experimental results with PEG and raffinose disappears since the end dimensions of PEG are smaller than the diameter of raffinose (Table 2). Therefore, PEG can sieve through any pore or slit with more ease than raffinose (Fig. 8).

To a first approximation, the upper limit in the dimensions of the structure where solutes are entrained by water must be about 0·6 nm, since molecules with a radius $r_m$ near or larger than 0·6 nm are not dragged and those with $r_m$ near or less than 0·55 nm are entrained. The lower limit for this structure must discriminate between markers that penetrate the cell (urea, erythritol, L-glucose and mannitol) and those that remain outside it (PEG and sucrose) (Table 1).

Therefore the cell membrane excludes molecules with an $r_m$ near or larger than 0·4 nm. The pathway where sucrose and PEG are entrained by water must therefore be twice 0·4–0·6 nm wide. This is illustrated in Fig. 8, which compares the dimensions of a 1·2 nm wide slit with those of the probes. It should be kept in mind that molecules excluded by the slit can still permeate the epithelium, in which case $P_0^s > 0$ because of the existence of alternative diffusive, but not convective, pathways.

Further quantification should follow steric hindrance theories (cf. Renkin & Curry, 1979): $\sigma = [1-(A_{sf}/A_{wf})]$ may be used. $A_{sf}$ and $A_{wf}$ are, respectively, the areas available for passage of solute and water during filtration. $A_{sf}$ may be written as a function of $(r_m/r_p)$, the ratio of the dimensions of the probe to those of the pore or slit, and $A_{wf}$ as a function of $(r_w/r_p)$, the ratio of the dimensions of water to those of the pore or slit. Such a treatment using the values of $\sigma$ (Table 2) indicates that a cylindrical pore of about 0·57 nm in radius and a slit with a half-width of 0·5 nm best fit the data. More precision is not possible at present because we have neither independent determinations of $\sigma$, nor a quantitative treatment for the sieving properties of rod-like molecules, nor enough information to be able to use equations for membranes in series and in parallel (cell membrane and intercellular space being in parallel and the septate and non-septate part of the intercellular spaces in series).

*Possible sites for paracellular solvent drag*

Fig. 9 depicts possible pathways for transepithelial water flow. In pathway 1, after crossing the cell membrane (possibly *via* aqueous pores, see Whittembury, Carpi, González & Linares, 1984) water would dissolve in the cytosol and would cross to the other end of the cell. Through this pathway water could, to some extent, drag small molecules that can cross the cell such as urea, erythritol, mannitol and L-glucose.

Pathway 2 is formed by the 15–20 $\mu$m long intercellular spaces which, in the Malpighian tubule, are formed by some 7 $\mu$m long smooth septate junctions in series with the rest of the intercellular space proper (Figs 6, 7). These junctions are known to let through $La^{3+}$ (Lane & Skaer, 1980), which is as big as $Na^+$ (Whittembury & Rawlins, 1971). Therefore, it is conceivable that water can also leak through. Through these pathways, water could drag only extracellular solutes like PEG and sucrose (and also the smaller probes mentioned above). A high degree of coupling between probes and solvent should not be surprising since, given the small relative frontal area of pathway 2, the speed of flow through these pathways should be very large.

Pathway 2a illustrates the structures described by Wessing (1965) and Bergeron *et al.* (1985) that extend from basolateral infoldings to cell apex. These structures appear in thin section electron micrographs as sets of parallel lines for such a length that they must represent sections of two parallel membranes forming slits (Figs 6, 7). They also appear as chains of vesicles or tubules (Bergeron *et al.* 1985). Since these structures are believed to open at both cell ends (Wessing, 1965), it is crucial at present to know whether these structures function as continuous pathways crossing the epithelium from base to apex. If that were the case, they could constitute a new pathway, effectively bypassing the cytosol where solvent drag could take place as in the intercellular pathway. An analogous possibility has been suggested as a pathway in some mammalian epithelia (Møllgård & Rostgaard, 1981). Pathways 2 and 2a would complement each other. However, pathway 2a must remain only hypothetical until further experiments prove or disprove it as an effective pathway.

In pathway 3, water could cross in vesicles or vacuoles. This pathway would explain neither the discrimination of the vesicles for the different probes (because it

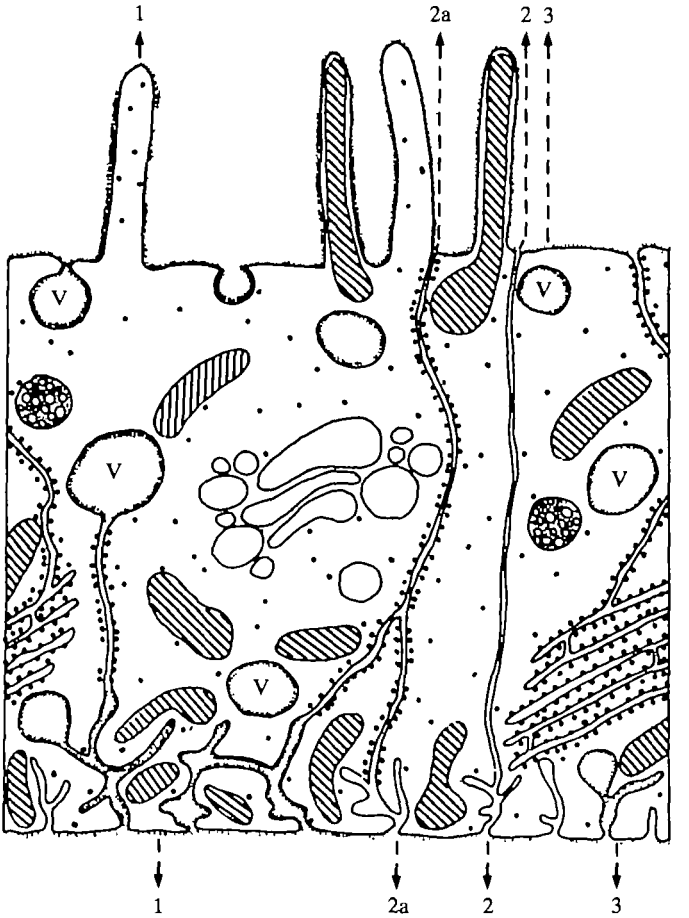


Fig. 9. Possible transepithelial water pathways: (1) transcytosolic; (2) paracellular (intercellular); (2a) through subcellular structures which shunt the cytoplasm from basal to apical membranes and (3) pathways that may use vacuoles (vesicles). Although 1 and 2a are both transcellular, 2a would bypass the cytosol and would function as a paracellular route. 3 may also bypass the cytosol by transient confluence of several vesicles.

would imply that some vesicles would have different contents of solutes), nor that inulin, dextran and raffinose are not dragged by water (unless the vesicles are connected with each other by narrow structures with characteristics similar to those already outlined for the pathway where solvent drag has been shown to occur). Calculations illustrate that the pathways for transepithelial water flow occupy only a small fraction of the epithelial area. This holds both for the possibility that all water flow is transcellular and for the extreme that it is all paracellular. The relative frontal area of the transcellular pathway, considering pores of about 0·4 nm in radius, would cover 0·6 % of the epithelial area; the paracellular pathway constitutes 0·08 % of the epithelial area (Whittembury *et al.* 1984, 1985).

It is a pleasure to thank Professor Josué Nuñez who developed the culture of *Rhodnius* and introduced us to the Malpighian tubule preparation. Mr José Mora,

Mrs D. Otero, Mr A. Cazorla, Mr Mardonio Díaz and Mr J. Bigorra helped in different stages of this research. Thanks are due to Mrs Rebeca Godoy and Elena Suárez for typing the manuscript. Miss A. Biondi's trip to Venezuela and her stay at IVIC were covered by Grants from Universidad de Tucumán and IVIC. This work constituted part of the Ph.Sc. thesis of A. Paz-Aliaga at the Centro de Estudios Avanzados, IVIC, Caracas. GW is also a member of Centro Internacional de Estudios Avanzados, IDEA, Caracas. Drs T. J. Pedley and G. K. Aldis kindly helped GW understand several of the unstirred layer problems involved.

## REFERENCES

ANDREOLI, T. E., SCHAFER, J. A. & TROUTMAN, S. L. (1971). Coupling of solute and solvent flows in porous bilayer membranes. *J. gen. Physiol.* **57**, 479–493.

BARRY, P. H. & DIAMOND, J. M. (1984). Effects of unstirred layers on membrane phenomena. *Physiol. Rev.* **64**, 763–873.

BERGERON, M., BERTHELET, F., BEAUDRY-LONERGAN, M., LINARES, H. & WHITTEMBURY, G. (1985). Morphological organization of the Malpighian tubule: endoplasmic reticulum as an epithelial transcellular route. *Kidney Int.* **27**, 323.

BERRY, C. A. (1983). Water permeability and pathways in the proximal tubule. *Am. J. Physiol.* **245**, F279–F294.

BERRY, C. A. & BOULPAEP, E. L. (1975). Nonelectrolyte permeability of the paracellular pathway in *Necturus* proximal tubule. *Am. J. Physiol.* **228**, 581–595.

BIONDI, A., LINARES, H., LINARES, N. & WHITTEMBURY, G. (1982). El agua arrastra solutos extracelulares durante la secreción en túbulos de Malpighi de *Rhodnius prolixus*. *Acta cientif. venezol.* **33**, suppl. 1, 193.

CARPI-MEDINA, P., LINDEMANN, B., GONZÁLEZ, E. & WHITTEMBURY, G. (1984). The continuous measurement of tubular volume changes in response to step changes in contraluminal osmolality. *Pflügers Arch. ges. Physiol.* **400**, 343–348.

CERF, R. & SCHERAGA, H. A. (1942). Flow birefringence in solution of macromolecules. *Chem. Rev.* **51**, 185–261.

CRANK, J. (1956). *The Mathematics of Diffusion*. Oxford: Clarendon Press.

DIAMOND, J. M. (1979). Osmotic water flow in leaky epithelia. *J. Membrane Biol.* **51**, 195–216.

FARQUHAR, M. G. & PALADE, G. E. (1963). Junctional complexes in various epithelia. *J. Cell Biol.* **17**, 375–412.

GONZÁLEZ, E., CARPI-MEDINA, P., LINARES, H. & WHITTEMBURY, G. (1984). Water osmotic permeability of the apical membrane of proximal straight tubular (PST) cells. *Pflügers Arch. ges. Physiol.* **402**, 337–339.

HILL, A. E. (1975). Solute–solvent coupling in epithelia. A critical examination of the standing gradient osmotic flow theory. *Proc. R. Soc.* B **190**, 99–114.

HILL, A. E. & HILL, B. S. (1978). Sucrose fluxes and junctional water flow across *Necturus* gall bladder epithelium. *Proc. R. Soc.* B **200**, 151–162.

HUNTER, M., CASE, R. M., STEWARD, M. C. & YOUNG, J. A. (1982). The permeability and reflection coefficients of the perfused rabbit mandibular salivary gland to non-electrolytes. In *Electrolyte and Water Transport Across Gastrointestinal Epithelia* (ed. R. M. Case, A. Garner, L. A. Turnberg & J. A. Young), pp. 21–32. New York: Raven Press.

JACOBS, M. H. (1935). Diffusion processes. *Ergebn. Biol.* **12**, 1–159.

KEDEM, O. & KATCHALSKY, A. (1958). Thermodynamic analysis of the permeability of biological membranes to nonelectrolytes. *Biochim. biophys. Acta* **217**, 229–246.

LANE, N. J. & SKAER, H. LE B. (1980). Intercellular junctions in insect tissues. *Adv. Insect Physiol.* **15**, 35–213.

MADDRELL, S. H. P. (1969). Secretion by the Malpighian tubules of *Rhodnius*. The movements of ions and water. *J. exp. Biol.* **51**, 71–97.

MADDRELL, S. H. P. (1980*a*). Characteristics of epithelial transport in insect Malpighian tubules. In *Current Topics in Membranes and Transport* (ed. F. Bonner & A. Kleinzeller), pp. 427–463. New York: Academic Press.

MADDRELL, S. H. P. (1980*b*). Bioassay of diuretic hormone in *Rhodnius*. In *Neurohormonal Techniques in Insects* (ed. T. A. Miller), pp. 81–90. New York: Springer-Verlag.

MADDRELL, S. H. P. & GARDINER, B. O. C. (1974). The passive permeability of insect Malpighian tubules to organic solutes. *J. exp. Biol.* **60**, 641–652.

MARTÍNEZ-PALOMO, A. & ERLIJ, D. (1975). Structure of tight junctions in epithelia with different permeability. *Proc. natn. Acad. Sci. U.S.A.* **72**, 4487–4491.

MØLLGÅRD, K. & ROSTGAARD, J. (1981). The transcellular compartment of tubulo-cisternal endoplasmic reticulum, a common feature of transporting epithelial cells. In *Water Transport Across Epithelia* (ed. H. H. Ussing, N. Bindslev, N. A. Lassen & O. Sten-Knudsen), pp. 85–101. Copenhagen: Munksgaard.

NOIROT-TIMOTHEE, C., SMITH, D. S., CAYER, M. L. & NOIROT, C. (1978). Septate junctions in insects: comparison between intercellular and intramembranous structures. *Tissue Cell* **10**, 125–136.

NOZAKI, Y., SCHECHTER, N. M, REYNOLDS, J. A. & TANFORD, C. (1976). Use of gel chromatography for the determination of the Stokes radii of proteins in the presence and absence of detergents: a reexamination. *Biochemistry, N.Y.* **15**, 3884–3890.

O'DONNELL, M. J., ALDIS, S. K. & MADDRELL, S. H. P. (1982). Measurements of osmotic permeability in the Malpighian tubules of an insect, *Rhodnius prolixus* Stal. *Proc. R. Soc.* B **216**, 267–277.

O'DONNELL, M. J. & MADDRELL, S. H. P. (1983). Paracellular and transcellular routes for water and solute movement across insect epithelia. *J. exp. Biol.* **106**, 231–253.

O'DONNELL, M. J., MADDRELL, S. H. P. & GARDINER, B. O. C. (1984). Passage of solutes through walls of Malpighian tubules of *Rhodnius* by paracellular and transcellular routes. *Am. J. Physiol.* **246**, R759–R769.

PAZ-ALIAGA, A., LINARES, H. & WHITTEMBURY, G. (1983). Flujo de agua por la vía paracelular en tubo de Malpighi. *Acta cient. venezol.* **34**, suppl. 1, 215.

PHELPS, C. F. (1965). Physical properties of inulin in solution. *Biochem. J.* **95**, 41–47.

RAMSAY, J. A. (1958). Excretion by the Malpighian tubules of the stick insect, *Dixippus morosus* (Orthoptera Phasmidae): aminoacids, sugars and urea. *J. exp. Biol.* **35**, 871–891.

RENKIN, E. M. (1970). Permeability and molecular size in 'peripheral' and glomerular capillaries. In *Capillary Permeability* (ed. C. Crone & N. A. Lassen), pp. 544–547. Copenhagen: Munksgaard.

RENKIN, E. M. (1985). Capillary transport of macromolecules: pores and other endothelial pathways. *J. appl. Physiol.* **58**, 315–325.

RENKIN, E. M. & CURRY, F. E. (1979). Transport of water and solutes across capillary endothelium. In *Membrane Transport in Biology*, vol. IVA (ed. G. Giebisch, D. C. Tosteson & H. H. Ussing), pp. 1–45. New York: Academic Press.

SCHAFER, J. A. (1984). Mechanisms coupling the absorption of solutes and water in the proximal nephron. *Kidney Int.* **25**, 708–716.

SCHLICHTING, H. (1979). *Boundary Layer Theory*. New York: McGraw Hill.

SHIPP, J. G., HANENSON, I. B., WINDHAGER, E. E., SCHATZMANN, H. J., WHITTEMBURY, G., YOSHIMURA, H. & SOLOMON, A. K. (1958). Single proximal tubules of the *Necturus* kidney. Methods for micropuncture and microperfusion. *Am. J. Physiol.* **195**, 563–569.

SKAER, H. LE B., HARRISON, J. B. & LEE, W. M. (1979). Topographical variation in the structure of the smooth septate junction. *J. Cell Sci.* **37**, 373–389.

STEWARD, M. C. (1982*a*). Paracellular non-electrolyte permeation during fluid transport across rabbit gall-bladder epithelium. *J. Physiol., Lond.* **322**, 419–439.

STEWARD, M. C. (1982*b*). Paracellular transport in the gall bladder. In *Electrolyte and Water Transport Across Gastrointestinal Epithelia* (ed. R. M Case, A. Garner, L. A. Turnberg & J. A. Young), pp. 1–10. New York: Raven Press.

WESSING, A. (1965). Die Funktion der Malpighischen Gefaesse. In *Funktionelle und Morphologische Organisation der Zelle: Sekretion und Exkretion* (ed. K. E. Wohlfarth-Bottermann), pp. 228–268. Berlin: Springer-Verlag.

WHITTEMBURY, G. (1967). Sobre los mecanismos de absorción en el túbulo proximal del riñón. *Acta cientif. venezol.* **18**, suppl. 3, 71–83.

WHITTEMBURY, G., CARPI-MEDINA P., GONZÁLEZ, E. & LINARES, H. (1984). Effect of pCMBS and temperature on cell water osmotic permeability of proximal straight tubules. *Biochim. biophys. Acta* **775**, 365–373.

WHITTEMBURY, G. & HILL, B. S. (1982). Fluid reabsorption by *Necturus* proximal tubule perfused with solutions of normal and reduced osmolarity. *Proc. R. Soc.* B **215**, 411–431.

WHITTEMBURY, G., PAZ-ALIAGA, A., BIONDI, A., CARPI-MEDINA, P., GONZÁLEZ, E. & LINARES, H. (1985). Pathways for volume flow and volume regulation in leaky epithelia. *Pflügers Arch. ges. Physiol.* **405**, Suppl. 1, S17–S22.

WHITTEMBURY, G. & RAWLINS, F. A. (1971). Evidence of a paracellular pathway for ion flow in the kidney proximal tubule: electronmicroscopic demonstration of lanthanum precipitate in the tight junction. *Pflügers Arch. ges. Physiol.* **330**, 302–309.

WHITTEMBURY, G., VERDE-MARTÍNEZ, C., LINARES, H. & PAZ-ALIAGA, A. (1980). Solvent drag of large solutes indicates paracellular water flow in leaky epithelia. *Proc. R. Soc.* B. **211**, 63–81.

WIGGLESWORTH, V. B. & SALPETER, M. M. (1962). Histology of the Malpighian tubules in *Rhodnius prolixus* (Hemiptera). *J. Insect Physiol.* **8**, 299–307.